Preparation and Characterization of Translocator/Chaperone Complexes and Their Component Proteins from *Shigella flexneri*†

Susan E. Birket,‡ Amanda T. Harrington,‡ Marianela Espina,‡ Nathan D. Smith,‡ Christina M. Terry,‡ Numukunda Darboe,‡ Aaron P. Markham,§ C. Russell Middaugh,§ Wendy L. Picking,‡ and William D. Picking*,‡

Departments of Molecular Biosciences and Pharmaceutical Chemistry, University of Kansas, Lawrence, Kansas 66045

Received January 17, 2007; Revised Manuscript Received April 12, 2007

ABSTRACT: *Shigella flexneri* causes a severe form of bacillary dysentery also known as shigellosis. Onset of shigellosis requires bacterial invasion of colonic epithelial cells which is initiated by the delivery of translocator and effector proteins to the host cell membrane and cytoplasm, respectively, by the *Shigella* type III secretion system (TTSS). The *Shigella* translocator proteins, IpaB and IpaC, form a pore complex in the host cell membrane to facilitate effector delivery; however, prior to their secretion IpaB and IpaC are partitioned in the bacterial cytoplasm by association with the cytoplasmic chaperone IpgC. To determine their structural and biophysical properties, recombinant IpaB/IpgC and IpaC/IpgC complexes were prepared for their first detailed *in vitro* analysis. Both IpaB/IpgC and IpaC/IpgC complexes are highly stable and soluble heterodimers whose formation prevents IpaB−IpaC interaction as well as Ipa-dependent disruption of phospholipid membranes. Circular dichroism spectroscopy shows that IpgC binding has a detectable influence on IpaC secondary/tertiary structure and stability. In contrast, IpaB structure is not as dramatically affected by chaperone binding. To more precisely ascertain the influence of chaperone binding on IpaC structure and stability, single tryptophan mutants were generated for detailed fluorescence spectroscopy analysis. These mutants provide a low-resolution picture of how IpaC exists in the *Shigella* cytoplasm with chaperone binding possibly involving distinct regions within the N- and C-terminal halves of IpaC. This preliminary assessment of the IpaC−IpgC interaction is supported by initial deletion mutagenesis studies. The data provide the first structural analysis of IpgC association with IpaB and IpaC.

The type III secretion system (TTSS)[1] is a virulence determinant used by a number of diverse Gram-negative bacterial pathogens (*1*). TTSSs are complex nanomachines that transport bacterial effector proteins into and across the cytoplasmic membranes of targeted eukaryotic cells (*2*). Although the proteins that make up the structural components of known TTSSs share some degree of sequence homology, the secreted effector proteins typically do not (*1*). The proteins initially secreted by TTSSs are the translocator proteins which form pores (translocons) in the host cell membrane to allow subsequent passage of effectors into the host cell cytoplasm (*3*). Prior to secretion, TTSS translocators and effectors are stored in the bacterial cytoplasm as complexes with their cognate chaperones (*4*). This interaction stabilizes the translocators and prevents their association prior to secretion (*4*). These chaperones probably also play a pivotal role in type III secretion by holding their partners in queue for secretion. After releasing their partners, some chaperones may interact with transcription factors to regulate late gene expression following the initial pathogen−host interaction (*5*).

Three classes of TTSS chaperones have been described with nearly all having low p*I*s and small molecular masses (*6*). Class I chaperones associate with one (subclass IA) or more (subclass IB) effectors that are targeted for the host cytoplasm. The slightly larger class II chaperones bind to the two translocator proteins that are associated with a given TTSS. Class III chaperones are specific to the flagellar TTSS. Class IA chaperones function as dimers with a significant β strand component (typically five strands) with three α helices per monomer which probably contribute to chaperone dimerization (*6*). Relatively little structural information is available for chaperones from the other classes.

Shigella flexneri, which causes a potentially severe form of dysentery called shigellosis, uses a TTSS to promote entry into human colonocytes. The *Shigella* invasive phenotype is encoded by the plasmid-borne *mxi/spa* operon, which encodes components of the type III secretion apparatus (TTSA), and the *ipa/ipg* operon, which encodes the translocator proteins IpaB and IpaC, and IpgC, which is the IpaB/IpaC-specific class II chaperone (*7*). IpgC prevents IpaB and IpaC from interacting in the cytoplasm prior to their secretion

† This work was supported by PHS Grants AI034428, RR017708 (CoBRE Protein Structure and Function Program), and AI057927 and the University of Kansas Research Development Fund to W.D.P.

* To whom correspondence should be addressed: Department of Molecular Biosciences, University of Kansas, 1200 Sunnyside Avenue, Lawrence, KS 66045. Tel: (785) 864-3299. Fax: (785) 864-5294. E-mail: picking@ku.edu.

‡ Department of Molecular Biosciences.

§ Department of Pharmaceutical Chemistry.

[1] Abbreviations: Ipa, invasion plasmid antigen; Ipg, invasion plasmid gene; TTSS, type III secretion system; TTSA, TTSS apparatus; IMAC, iminodiacetic; Trp, tryptophan; DOPC, 1,2-dioleoyl-*sn*-glycero-3-phosphocholine; DOPG, 1,2-dioleoyl-*sn*-glycero-3-[phospho-*rac*-(1-glycerol)]; OPOE, *n*-octyl-polyoxyethylene; SRB, sulforhodamine B; DSP, dithio-bis-(succinimidylpropionate); DTT, dithiothreitol; CD, circular dichroism; DLS, dynamic light scatter; AUC, analytical ultracentrifugation; SEC, size exclusion chromatography.

10.1021/bi700099c CCC: $37.00
Published on Web 06/16/2007

(*4*), and it may hold them in a secretion-competent conformation. Upon host cell contact, the *Shigella* TTSS inserts IpaB and IpaC into the host cell membrane to form a pore that permits passage of other *Shigella* effectors into the host cell cytoplasm (*8*, *9*). Unlike translocators of other TTSSs, IpaB and IpaC are also implicated in directly triggering signaling events. IpaB induces apoptosis in macrophages (*10*), and IpaC triggers cytoskeletal rearrangements in macrophages and epithelial cells that promote bacterial entry (*11*−*13*).

Because of their overall apolar nature, recombinant IpaB and IpaC have proven difficult to purify (*11*, *14*). IpaC behaves as a membrane protein with two predicted transmembrane domains located within a larger nonpolar region that renders the protein insoluble during purification. In the case of IpaB, stability and solubility present major purification obstacles (*14*). Both proteins, however, are maintained in a soluble state in the *Shigella* cytoplasm due to their association with IpgC (*4*). Thus, in this work *ipaB* or *ipaC* was coexpressed with *ipgC* in *Escherichia coli* to produce high yields of soluble IpaB/IpgC and IpaC/IpgC complexes that are easily purified via a His_6 tag located at the IpgC N-terminus. Once purified, IpaB or IpaC can be released from IpgC by mild detergent and low pH, respectively. In this study, the purification and biophysical properties of the complexes and their individual components are described. The implications these findings have with respect to the delivery of translocon/effector proteins to target cells are also discussed.

MATERIALS AND METHODS

Materials. The pACYCDuet-1 plasmid, 2X Ligation Premix, and *E. coli* strains were from Novagen (Madison, WI). Superdex 200 gel filtration columns were from Amersham Biosciences (Piscataway, NJ). Iminodiacetic acid (IMAC)-Sepharose was from Sigma Chemical Co. (St. Louis, MO). Dioleoylphosphatidylcholine (DOPC), dioleoylphosphatidylglycerol (DOPG), and cholesterol were from Avanti (Alabaster, AL). Sulforhodamine B (SRB) was from Molecular Probes (Eugene, OR) and *n*-octyl-polyoxyethylene (OPOE) from Alexis Biochemical (Lausen, Switzerland). All other chemicals were reagent grade. The *S. flexneri ipaC* null mutant strain SF621 was obtained from P. Sansonetti (Institut Pasteur).

Generation of Plasmids for Expression of the ipa Genes in E. coli. The pET15b plasmid containing *ipgC*, pWPipgC, has been described (*15*). The pACYC-C plasmid was generated by PCR using a 5′ primer containing GAGAGA, a *Nde*I restriction site, and 18 bases complementary to the 5′ end of *ipaC*, a 3′ primer containing GAGAGA, a *Xho*I site, and 18 bases complementary to the 3′ end of *ipaC*, and pWPC15 as template DNA (*14*). The PCR product was digested with *Nde*l and *Xho*I, ligated into pACYCDuet-1, and transformed into *E. coli* NovaBlue. The pACYC-B plasmid was similarly produced except that a *Kpn*I site was used at the 3′ primer with pWP15B as template (*14*). The pACYC-C trp mutants were amplified from plasmid templates described elsewhere using a 3′ primer containing a *Kpn*I site (*16*). For coexpression, pACYC-B or -C and pWPipgC were co-transformed into *E. coli* Tuner(DE3) using ampicillin and chloramphenicol to select for both plasmids. The preparation of IpaC single Trp mutants was performed as described (*16*). Whenever possible, the inserted Trp residues were used to replace bulky hydrophobic residues such as lysine, phenylalanine, or isoleucine, but this was not always possible. Thus, all mutants were used to determine whether they still possessed native function by complementing a *Shigella ipaC* null mutant (*16*). The IpaC internal deletion mutant $IpaC^{\Delta 1-20/\Delta 177-259}$ (designated IpaCΔ here) was generated in the same manner as previously described (*17*) and subcloned into pACYCDuet-1.

Purification of Recombinant Proteins. IpaC was prepared as previously described (*11*, *17*). Tuner(DE3) cells containing pACYC-C/pWPipgC (or *ipaC* mutants) or pACYC-B/pWPipgC were grown as previously described (*15*, *17*). The bacterial suspension was sonicated, and centrifuged for 15 min at 27000*g*. The clarified supernatant was loaded onto a 10 mL charged IMAC-Sepharose column and washed with binding buffer and the protein eluted with buffered 1 M imidazole (*14*). Protein fractions were pooled and EDTA and dithiothreitol (DTT) added to a final concentration of 1 mM and 0.5 mM, respectively. The protein was loaded onto a HiLoad 26/60 Superdex 200 preparative grade column equilibrated with 10 mM Tris-HCl pH 7.2, 150 mM NaCl, 0.5 mM DTT (TBS/DTT) to separate the complex from free IpgC by size exclusion chromatography (SEC). Molecular mass was estimated using the protein standards carbonic anhydrase (29 kDa), bovine serum albumin (66 kDa), yeast alcohol dehydrogenase (150 kDa), and β-amylase (200 kDa). The complexes were stored at −70 °C. Protein concentrations were determined by measuring the absorbance at 280 nm using extinction coefficients based on the amino acid composition of each protein (*18*).

Dissociation of Protein in Complexes. Dissociation of the IpaC/IpgC complex was achieved by dialysis against TBS/DTT at pH 5.0. The free IpaC was isolated using the HiLoad 16/60 Superdex 200 preparative grade column equilibrated with TBS/DTT (pH 5.0). The sample was then dialyzed against Tris-buffered saline (pH 7.2) to bring it into a more physiologically relevant environment for storage at −80 °C and biophysical characterization. The IpaB/IpgC complex could be dissociated by the addition of OPOE to 2%. The protein solution was then passed over a charged IMAC column collecting the free IpaB in the flow through. The OPOE was removed by extensive dialysis against TBS. The proteins were stored at −70 °C.

Cross-Linking of Protein Complexes. Dithio-bis-(succinimidylpropionate) (DSP), a homobifunctional, amine-reactive, thiol-cleavable cross-linking agent (*19*), was used to reversibly cross-link the Ipa/IpgC complexes to initially determine their stoichiometry. DSP in *N*,*N*-dimethylformamide (DMF) was added to a 2 mg/mL protein complex solution to yield a final concentration of 3.75 mM. After 30 min, the reaction was stopped by the addition of SDS−PAGE sample buffer with or without 50 mM DTT. Samples were then subjected to SDS−PAGE.

Analytical Ultracentrifugation (AUC). Sedimentation velocity experiments were performed with a Beckman Proteolab XL-1 analytical ultracentrifuge equipped with scanning UV/visible optics. An AN 50ti 4-hole rotor and preassembled cells were used and sedimentation coefficients obtained at a single concentration (2 mg/mL) at 25 °C. Samples were spun at 25,000 rpm and scanned every 10 min for 10 h. Data was

analyzed using SEDFIT version 9.3b (http://dbeps.ors.od-.nih.gov/pbr_AUCsedfit.htm). Partial specific volumes were calculated employing SEDNTERP version 1.09. The data was analyzed as a continuous distribution. The molecular weight of the protein was determined using the value of the diffusion coefficient determined by DLS.

Dynamic Light Scattering (DLS). To provide a preliminary measure of the hydrodynamic radius of the IpaC/IpgC complex, dynamic light scattering (DLS) was employed. Light scattering studies were conducted with a Brookhaven system consisting of a 50 mW HeNe diode laser operating at 532 nm, a BI-200SM goniometer with an EMI 9863 PMT, and a BI9000AT autocorrelator. Experiments were conducted at a protein concentration of 1 mg/mL at multiple angles. Experiments were repeated 3 times with final values of the hydrodynamic radius and polydispersity determined by cumulant analysis with an accompanying standard error. The experiments were performed in an environment that minimized dust interference. Using this system, size determinations are obtained with a precision and accuracy of >3% with monodisperse particles over a size range of 0.002−1 μm.

Preparation of Phospholipid Vesicles. Aliquots of DOPC, DOPG, and cholesterol in chloroform were dried under nitrogen and vacuum for 3 h to create lipid films of 14:5:1 [DOPC]:[DOPG]:[cholesterol]. Lipid films were hydrated in water containing 100 mM sulforhodamine B (SRB), sonicated for 10 s, and extruded through a 100 nm pore size membrane 10 times at 45 °C. Excess dye was separated from the liposomes by gel filtration using Sephadex G-50 equilibrated with 10 mM phosphate (pH 7.2), 150 mM NaCl. Peak fractions were pooled, stored at 4 °C, and used within one week.

Monitoring Rhodamine Release from Phospholipid Vesicles. SRB release from phospholipid vesicles was monitored using a SPEX FluoroMax spectrofluorometer. After an initial baseline of fluorescence from the liposomes was established, protein was added and SRB release detected as an increase in fluorescence intensity over time. As a control for complete SRB release, 0.1% Triton X-100 was added, while the *Shigella* protein IpaD was used as a negative control.

Circular Dichroism Spectroscopy of Proteins and Protein Complexes. Far-UV CD spectra and thermal unfolding monitoring at 222 nm were performed using a Jasco J720 spectropolarimeter (Jasco Inc., Easton, MD). Far-UV spectra were recorded from 190 to 260 nm at a scan rate of 15−20 nm/min employing a 0.01 cm path length cell with spectra acquired in triplicate and averaged. The thermally induced unfolding transitions were acquired using a 0.1 cm path length cell with a temperature ramping rate of 15 °C/h. Protein concentrations ranged from 1 to 10 μM with all experiments performed in PBS or phosphate buffer (pH 7.2) to minimize pH shifts induced by temperature. CD signals were converted to molar ellipticities, and the unfolding transitions were analyzed using the Jasco Spectral Manager software (*11*).

Fluorescence Spectroscopy. Fluorescence emission spectra were acquired using a PTI QM-1 spectrofluorometer (Monmouth Junction, NJ) equipped with Felix software. Using a 1 cm path length cell, samples were excited at 295 nm (>95% Trp excitation) and the emission spectra collected from 305 to 400 nm at a scan rate of 30 nm/min. For thermal transitions, spectra were taken at 2.5 °C temperature intervals with each spectrum an average of two scans. A buffer spectrum was subtracted from the sample spectrum at the corresponding temperature. Based on protein concentration, slit widths were set between 4 and 6 nm. For determination of emission maxima in the presence and absence of liposomes, spectra were obtained using a Spex FluoroMax spectrophotometer.

RESULTS

Purification of Complexes Composed of IpgC and IpaC or IpaB. To mimic conditions in the *Shigella* cytoplasm where IpgC maintains the IpaB and IpaC translocators as soluble protein complexes, a plasmid encoding IpgC was cotransformed into *E. coli* with a plasmid expressing one or the other of the translocator proteins. Coexpression of IpaC or IpaB with His-tagged IpgC permits the production of soluble IpaC/IpgC and IpaB/IpgC complexes in large quantities. After conventional IMAC column chromatography, the translocator/chaperone complexes were separated from free chaperone by SEC (Figure 1). Based on migration relative to proteins of known mass (see Materials and Methods), the IpaC/IpgC complex migrates with an apparent molecular mass of 121 kDa while the free IpgC migrates at about 45 kDa (Figure 1A and 1C). The IpaB/IpgC complex migrates with an apparent molecular mass of 144 kDa (Figure 1A and 1B). Given that the molecular mass of IpaC is 41 kDa and IpgC is 20 kDa, free IpgC appears to migrate as a dimer and the migration of the IpaC/IpgC complex may be explained by the presence of an $IpaC_2$:$IpgC_2$ complex, but this requires confirmation. Such a 2:2 stoichiometry might also be proposed for the IpaB/IpgC complex since both are anticipated to interact with IpgC in a conserved manner. The IpaB/IpgC complex, however, does not behave precisely in this manner. The theoretical molecular mass of IpaB is 62 kDa, which would suggest that a complex with a 2:2 stoichiometry with IpgC would migrate with an apparent molecular mass of 160 kDa. This is approximately 16 kDa more than that observed (Figure 1).

Determination of Complex Sizes by Biochemical and Biophysical Methods. To initially determine the stoichiometry of the translocator/chaperone complexes, the thiol-cleavable cross-linker DSP was used. After DSP treatment, IpaC/IpgC and IpaB/IpgC were subjected to SDS−PAGE with or without DTT (Figure 2). The IpaC/IpgC and IpaB/IpgC complexes migrated with apparent masses of 60 kDa and 80 kDa, respectively (Figure 2), with no staining in the 140−160 kDa regions. These data are consistent with a translocator to chaperone stoichiometry of 1:1. After treatment with 50 mM DTT, the translocators and chaperone again migrate as monomers (Figure 2). Previously, mass spectrometry analyses also indicated a 1:1 ratio for the distantly related PopB/PcrH and PopD/PcrH translocon and chaperone pairs of *Pseudomonas aeruginosa* (*20*). Thus, the larger than expected size, based on SEC, for the IpaB/IpgC and IpaC/IpgC complexes may indicate that they are asymmetric in shape.

To confirm the size of the translocator/chaperone complexes, sedimentation velocity analysis was used. It indicated that the IpaC/IpgC complex has a molecular mass of 59.7 ± 1.8 kDa (n = 3), which agrees well with the theoretical

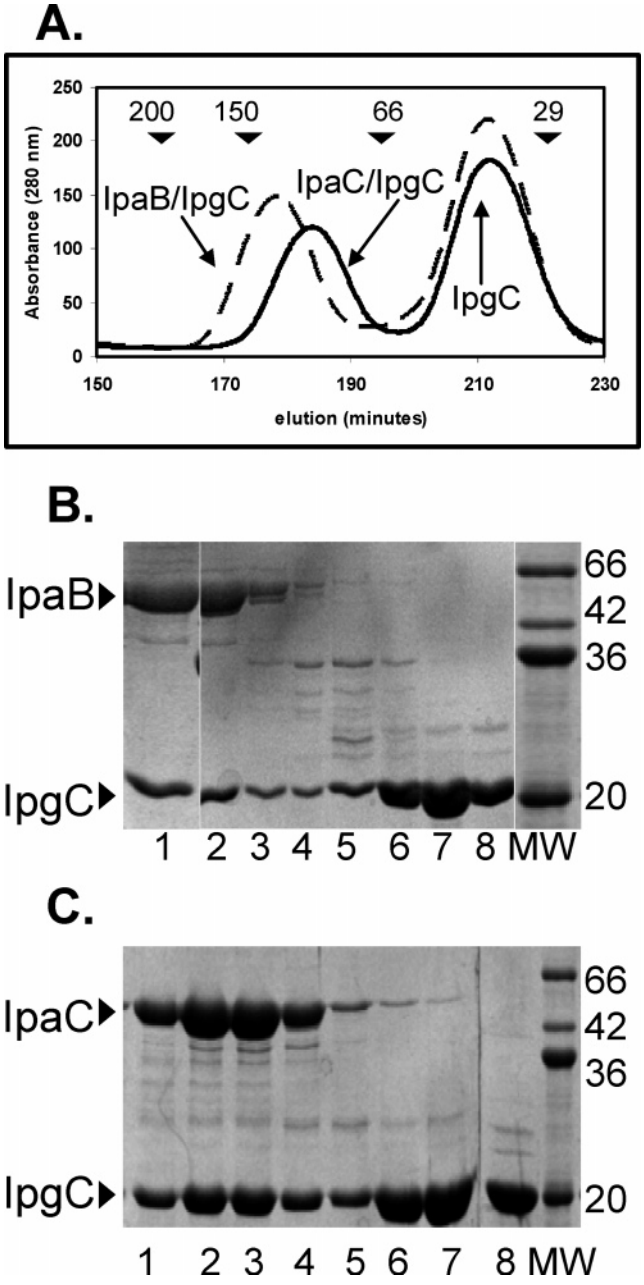

FIGURE 1: Purification of IpaB/IpgC and IpaC/IpgC complexes by gel filtration. Following IMAC affinity chromatography, the soluble translocator/chaperone complexes were separated from free chaperone by Superdex S-200 26/60 column chromatography. Panel A shows the S-200 chromatograms of IpaB/IpgC (− − −) and IpaC/IpgC (−). Molecular masses of the protein standards used for calibration are indicated with arrows at the top. The void volume for this column is 105 min. Panels B and C are the Coomassie Blue stained SDS−PAGEs of the IpaB/IpgC and IpaC/IpgC fractions, respectively. In both panels, the last lane shows molecular weight markers of 66, 40, 35, and 20 kDa.

size of an IpaC/IpgC complex with a 1:1 stoichiometry (41 kDa + 19 kDa for IpaC and IpgC, respectively). Similarly, this method finds that the IpaB/IpgC complex has a molecular mass of about 81 kDa. These results also support the cross-linking data that indicate a 1:1 stoichiometry rather than the 2:2 stoichiometry suggested by SEC. In each case the frictional ratio (f/f_0) (a measure of asymmetry based on the measured frictional coefficient and that calculated for a hypothetical sphere) was about 1.7, indicating that the protein complexes are indeed highly elongated.

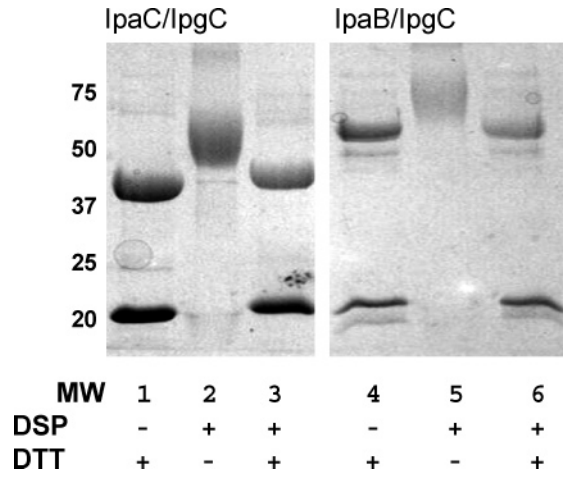

FIGURE 2: Cross-linking of IpgC-containing protein complexes. Purified IpaC/IpgC and IpaB/IpgC complexes were subjected to cross-linking with DSP and separated by SDS−PAGE with or without 50 mM DTT. After the molecular marker lane, lanes 1−3 are IpaC/IpgC with (+) and without (−) DSP and with (+) or without (−) DTT. Lanes 4−6 are IpaB/IpgC with (+) and without (−) DSP and with (+) or without (−) DTT.

Dynamic light scattering (DLS) was then used to show that the IpaC/IpgC complex was monodisperse in solution and had an apparent hydrodynamic radius of 9.7 ± 0.3 nm, which is similar to that seen for the IpaB/IpgC complex. The absence of polydispersity for both protein complexes (greater than 95% monodisperse) suggests that they are not immediately prone to aggregation. For each protein complex, the expected diameter, if spherical, would be about 6 nm, again suggesting that the complexes are elongated ($f/f_0 \sim 1.6$).

Separation of IpaC and IpaB from Their Protein Complexes. To separate IpaC from its complex with IpgC, the pH of the solution was lowered to 5.0, a method used to separate the *P. aeruginosa* PopD/PcrH complex (*20*). During SEC, the released IpaC migrated with an apparent molecular mass of approximately 235 kDa with no chaperone detected within this complex (see Figure 3). This IpaC oligomer, which forms after separation from IpgC at pH 5, remained intact after exchange into buffered saline at pH 7.2. Whether this high molecular weight oligomer represents the actual physiological "oligomeric state" of IpaC is not yet known, but this is intuitively attractive and provides additional evidence of IpaC's ability to oligomerize to a specific size in solution (*17*, *21*).

In contrast to the *P. aeruginosa* PopB/PcrH complex (*20*), IpaB was not released from IpgC by lowering the pH (data not shown). This suggests that the IpaB/IpgC complex involves a different set of intermolecular interactions relative to the IpaC/IpgC complex. Purification of IpaB from *E. coli* in the absence of the chaperone requires detergent (*22*). Therefore, the IpaB/IpgC complex was treated with the mild detergent OPOE which released IpaB from the complex. Released IpaB passed through the IMAC column while free IpgC and the remaining complex bound. When passed over the Superdex 200 column, IpaB eluted in the void volume, indicating the presence of a soluble high molecular weight aggregate lacking chaperone. Addition of OPOE to the IpaC/IpgC complex did not cause release of IpaC (data not shown), again suggesting that IpaB and IpaC associate with IpgC using a different repertoire of interactions.

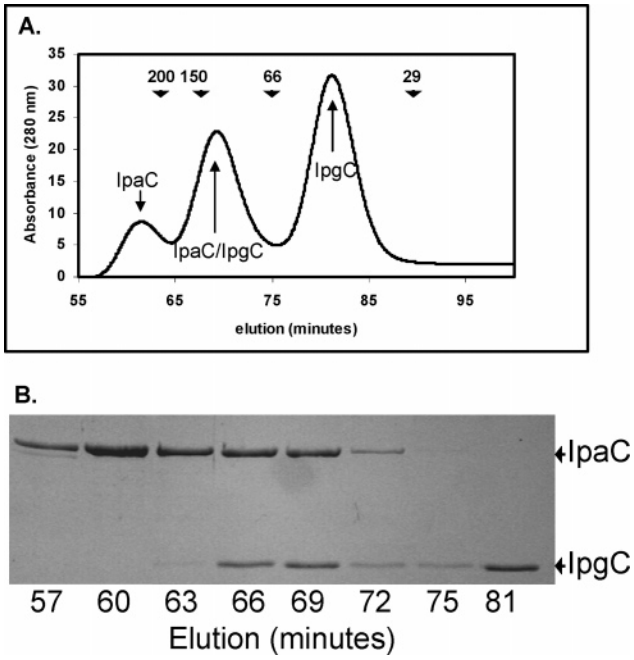

FIGURE 3: Separation of IpaC from IpaC/IpgC complexes after low pH treatment by passage over a Superdex S-200 16/60 gel filtration column. Panel A shows the S-200 chromatogram. The void volume for this column is 40 min. Panel B shows the SDS−PAGE profile of IpaC separated from IpaC/IpgC complexes and free IpgC. No protein staining was observed in the 140−160 kDa range or within the stacker portion of the gels.

Interaction of Proteins and Protein Complexes with Phospholipid Membranes. It has been previously shown that both IpaB and IpaC can interact with and disrupt phospholipid membranes (*11*, *16*, *22*). The ability of the translocator/chaperone complexes to interact with membranes was assessed by a membrane-disruption assay using SRB encapsulated in unilamellar phospholipid vesicles composed of 70% DOPC, 25% DOPG, and 5% cholesterol (*11*, *16*, *23*). Free IpaC and IpaB cause release of SRB from liposomes while IpaB and IpaC in complexes with IpgC, as well as purified IpaD (negative control), do not (Figure 4). We have shown that cholesterol can negatively affect IpaC's interaction with liposomes (*16*). The IpaC/IpgC complex, however, did not allow SRB release from liposomes lacking cholesterol or containing up to 50% of an acidic phospholipid (data not shown). These data show that IpgC interaction with IpaC and IpaB has an inhibitory effect on their ability to disrupt liposomes.

Far-UV Circular Dichroism Determination. The far-UV CD spectra of IpgC, IpaB, IpaC, and translocator/chaperone complexes (Figure 5) suggest that IpaC, but not necessarily IpaB, undergoes a noticeable change in secondary structure content when it is released from its chaperone. To estimate secondary structure content, the spectra were analyzed by Dichroweb (Table 1) (*24*, *25*). When the experimentally determined secondary structure of the binary complexes is compared to the predicted secondary structure content (calculated from individual spectra of the purified proteins), these analyses confirm that chaperone association induces substantial structural change in IpaC, but not in IpaB. For example, the sum of the α-helical content observed for IpaC and IpgC individually is actually less than that observed for the complex while the overall amount of β-structure decreases as the complex is formed, suggesting a significant

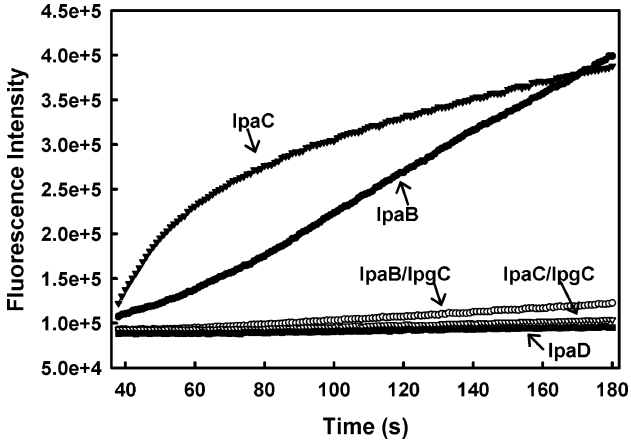

FIGURE 4: Interaction of purified Ipa proteins and Ipa/IpgC protein complexes with phospholipid membranes. IpaB and IpaC alone and complexed with IpgC were incubated at pH 7.2 with unilamellar liposomes containing SRB. Release of the SRB, caused by disruption of the membrane bilayer, is indicated by an increase in fluorescence intensity as a function of time. IpaD serves as the negative control since this protein is highly soluble and is not expected to interact with phospholipid membranes. The approximate Ipa protein concentration in each case is 1 μM. The purified IpaC in these experiments was maintained at high concentrations as a stock solution in 2 M urea. The addition of urea alone had no effect on the SRB-containing liposomes (data not shown).

conformational difference (Table 1). These features can also be discerned from the spectra shown in Figure 5. The decrease in β strand content suggests that the loss of β-structure is compensated by an increase in α-helix content upon IpaC association with its chaperone. These findings suggest that IpaC is more ordered when associated with IpgC than when alone, and this is supported by trypsinolysis data showing that IpaC is rapidly hydrolyzed to completion while IpgC-associated IpaC is hydrolyzed more slowly with the formation of stable intermediates of about 26 kDa and 30 kDa in size (see Supporting Information Figure S1). In contrast, there is less change in the secondary structure of IpaB and IpgC when these two proteins form their binary complex (Figure 5B and Table 1).

When an IpaC deletion mutant IpaC$^{\Delta 1-20/\Delta 177-259}$ (designated IpaCΔ) was generated in a complex with IpgC and the CD spectrum obtained, a decrease in α-helix content suggested that structured regions of IpaC were missing from the complex (see Figure 5A); however, this form of IpaC still retained those regions needed for stable chaperone binding. IpaCΔ lacks an N-terminal TTSS secretion signal that is not expected to be highly structured and a central polar region (residues 177−259) that is not needed for IpaB/IpaC pore formation in target cells (*17*). The fact that this IpaC deletion mutant still forms a stable complex with IpgC shows that this central region can be deleted without a negative impact on chaperone interaction even though it lacks the N-terminal region needed to target it for type III secretion. Larger N-terminal deletions (beyond residue 50) or large C-terminal deletions do prevent the copurification of IpaC with its chaperone (data not shown). It is worth noting that the stable IpaCΔ/IpgC complex has less overall helical structure than does the IpaC/IpgC complex (25% versus 53%, respectively). One could speculate that this is initial evidence that IpgC binding influences the structure of IpaC regions that are not directly involved in chaperone binding.

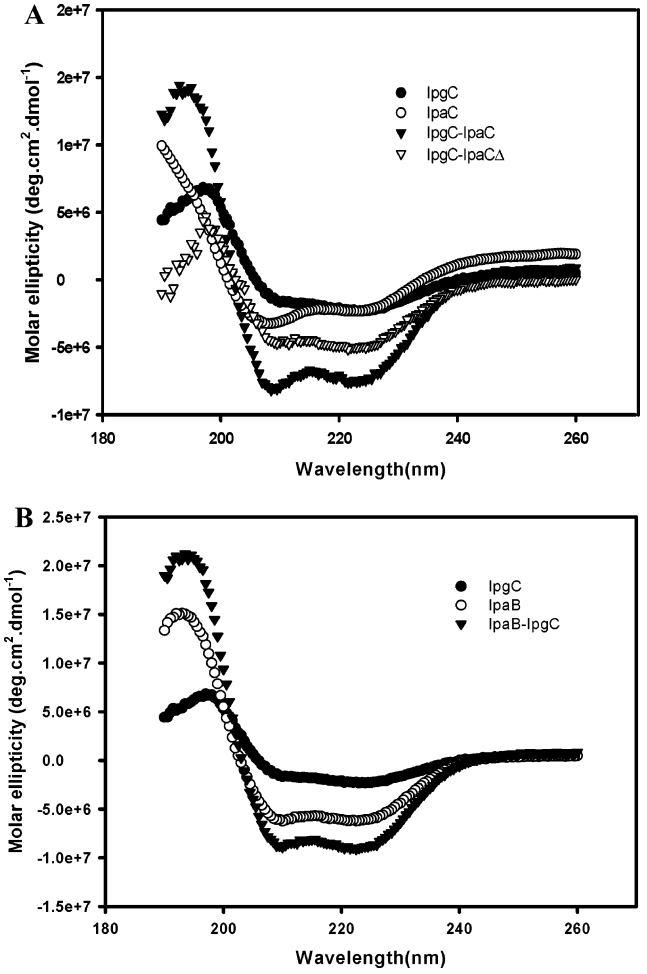

FIGURE 5: Far-UV CD spectra of purified proteins and protein complexes. Far-UV CD spectra are overlaid for IpaC (5 μM), IpgC (20 μM), IpaC/IpgC (11.3 μM), and IpaCΔ/IpgC (10 μM) (panel A) and IpaB (20 μM), IpgC (20 μM), and the IpaB/IpgC (12.7 μM) (panel B). These spectra are an average of two representative CD spectra.

Table 1: Deconvolution of the Far-UV CD Spectra for IpaB, IpaC and IpgC[a]

protein	α-helix	β-sheet	turns	random
IpgC	0.52	0.21	0.11	0.17
IpaB	0.42	0.15	0.16	0.28
IpaB + IpgC[b]	0.46	0.18	0.13	0.22
IpaB/IpgC[c]	0.46	0.14	0.15	0.27
IpaC	0.30	0.23	0.18	0.31
IpaC + IpgC[b]	0.42	0.22	0.14	0.24
IpaC/IpgC[c]	0.53	0.08	0.12	0.28

[a] Deconvolution of the far-UV spectra into various secondary structure elements was performed using SELCON and CONTIN algorithms (*32*, *33*). The values are the averages between the two methods, which are in excellent agreement with each other. The estimated uncertainty in these values is about ±0.03. [b] The calculated or theoretical sum of the percentage of secondary structure elements from the individual proteins. [c] The experimentally determined secondary structure element (following deconvolution) of the binary complex is based on the CD spectra shown in Figure 5.

Assessment of the Local Trp Environments of IpaC Single-Tryptophan Mutants Using Fluorescence Spectroscopy. CD spectroscopy clearly indicates that IpaC's structure is influenced by association with IpgC. To determine how IpgC affects the microenvironment of regions within IpaC, specific local environments were monitored based on Trp fluorescence. Since there are no Trp residues in IpaC or in IpgC, substitutions were made at several strategic points in IpaC (Figure 6): position 40 near the IpaC N-terminal region that is responsible for secretion, chaperone binding, and IpaB binding (*15*); positions 106, 136, and 154 within the central hydrophobic region required for structural stability (*11*) and membrane interactions (*17*); positions 195, 207, 226, 247, and 270 located within the central hydrophilic domain (*17*); positions 336 and 341 located within the predicted coiled-coil trimerization domain necessary for IpaC oligomerization (*11*, *26*); and the penultimate C-terminal residue (position 362) which is important for effector function (Flentie, K., and Picking, W., unpublished data). IpaB complexes were not examined here by Trp mutagenesis because IpaB already possesses a single Trp residue which would complicate further analysis. The wavelength emission maximum of the Trp fluorescence was determined for each protein and for the translocator/chaperone complexes. Because the indole group of Trp is very environmentally sensitive, predictions about the polarity of the environment of each Trp based on its fluorescence properties can be made. Thus, a spectral shift to a lower wavelength (blue shift) typically indicates movement of the Trp into a more nonpolar environment. Fluorescence of the Trp residues at positions 40, 207, 226, 247 undergo a small blue shift (<4 nm) while Trp residues at positions 106, 154, 336, and 362 undergo more dramatic blue shifts (>4 nm) when the protein is associated with IpgC (Table 2). In contrast, Trp residues located at positions 136 and 341 undergo minor red shifts, indicating movement into a more polar environment upon complex formation. The data suggest that there is a strong influence of IpgC binding on the hydrophobic region and parts of the IpaC C-terminus. Trp fluorescence intensity changes appeared to mirror changes in emission maximum (with blue shifts typically accompanied by increases in intensity); however, the emission maxima provided a more reliable measure of environmental changes due to independence from overall protein concentration.

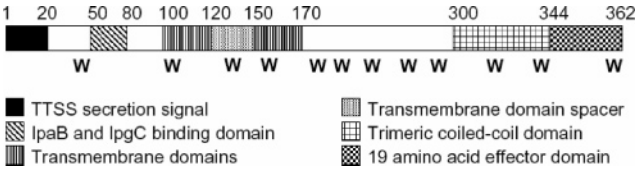

FIGURE 6: Schematic diagram of regions of IpaC and the location of the substituted Trp residues. The beginning and ending amino acid residues of each region are indicated above the diagram. W represents the location of each substituted Trp residue. Residues 1−20 encode a TTSS secretion signal. Residues 50−80 are necessary for IpgC binding and interaction with IpaB. Residues 100−170 encode the transmembrane domain with residues 120−150 forming the loop between the two domains. Residues 300−344 encode the putative trimeric coiled-coil. Residues 345−362 encode a 19-amino acid "tail" involved in IpaC effector function. In order, the shown Trp residues are at positions 40, 106, 136, 154, 195, 207, 226, 247, 270, 336, 341, and 362.

Thermally Induced Unfolding Monitored by CD and Fluorescence Spectroscopy. To further examine the influence of chaperone binding on the structure of IpaC, thermally induced unfolding of the individual proteins and their binary complexes was monitored by both CD and fluorescence spectroscopy (Table 3 and Figure 7). The CD profile was monitored at 222 nm to probe α-helical content changes

Table 2: Emission Maxima for IpaC Single Trp Mutants in Complex with IpgC

Trp mutant	Em_{max} [a,b,c]	Em_{max} with IpgC[b]	ΔEm_{max}
IpaC[d]	na	na	na
I40W	344.0	340.7	−3.3
A106W[e]	**342.5**	**335.7**	**−6.8**
F136W	342.9	343.7	0.8
L154W	**342.2**	**327.0**	**−15.2**
L195W	**349.5**	**344.0**	**−5.5**
L207W	349.0	345.2	−3.8
L226W	347.2	344.5	−2.7
L270W	347.2	347.2	0.0
L247W	349.1	347.0	−2.1
I336W	**345.7**	**337.3**	**−8.4**
N341W	344.3	348.0	+3.7
R362W	**344.2**	**334.7**	**−9.5**

[a] Fluorescence emission maxima are presented as wavelength in nm. [b] $n \geq 3$, and the precision of the peak position measurements is estimated to be ±0.3 nm. [c] IpaC purified as previously described (*11*) or by pH-dependent release from IpaC/IpgC complexes has nearly identical emission maxima (data not shown). [d] Wild-type IpaC possesses no Trp residues and therefore these data are not available. [e] Boldface indicates mutants that have a substantial blue shift in the chaperone bound protein versus free IpaC.

Table 3: Thermally Induced Unfolding of IpaC, IpgC, and IpgC with Selected Single Trp Mutants

protein	CD T_m ± SE, °C	ΔT_m[a]	FL,[b] °C
IpgC	53.9 ± 0.2	na	na
IpaC	45.5 ± 0.3	0	na
IpaC/IpgC	56.3 ± 0.1	10.8	na
W40/IpgC	56.2 ± 0.2	10.7	**53**
W106/IpgC	55.0 ± 0.1	9.5	58
W136/IpgC	56.1 ± 0.1	10.6	58
W154/IpgC	54.5 ± 0.4	9.0	55
W195/IpgC	57.8 ± 1.8	12.3	60
W207/IpgC	54.9 ± 1.6	9.4	**40**
W226/IpgC	57.0 ± 0.9	11.5	**51**
W247/IpgC	56.7 ± 1.0	11.2	**54**
W270/IpgC	56.9 ± 0.2	10.5	62
W336/IpgC	54.5 ± 0.2	9.0	56
W341/IpgC	53.0 ± 0.1	7.5	**51**
W362/IpgC	57.2 ± 0.2	11.7	57

[a] Change in the CD T_m is relative to IpaC in the absence of IpgC. [b] The fluorescence data provided are an estimate of the midpoint of transition with $n = 3$.

while the fluorescence profile was analyzed at 340 to capture tertiary structure alterations (Figure 7). The CD spectra show a cooperative transition from a folded conformation to a structurally disrupted form. In all cases, the pre- and post-transition baselines were well-defined with a clearly defined midpoint of the thermal transition (T_m). This permitted precise T_m determinations for both the individual proteins and the translocator/chaperone complexes (Table 3). All of the CD-based T_m values fall within 3 °C of each other with one outlier (W195) also demonstrating the greatest degree of experimental error. This suggests only a relatively minor impact of Trp substitution on global secondary structure and stability. Another outlier (W341) is within a presumably exposed region of the IpaC−IpgC complex, and its unexpectedly low T_m is not yet understood.

Unlike CD spectroscopy, which provides a global picture of secondary structure content, the fluorescence spectra of the different IpaC single Trp mutants provide an assessment of more localized effects. Thus, the Trp fluorescence-based

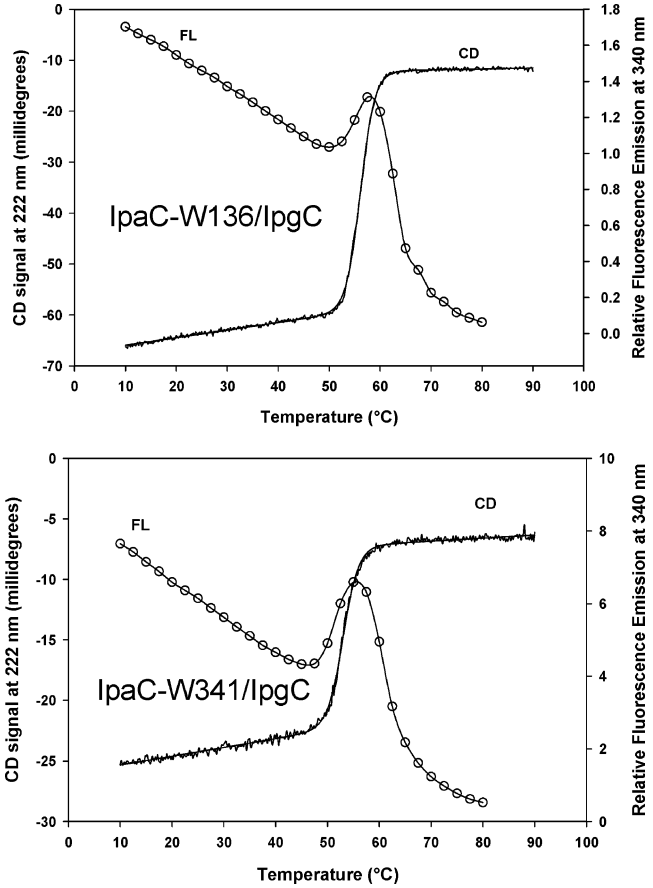

FIGURE 7: Representative curves showing the thermally induced unfolding for IpgC-containing complexes. In each panel, the open symbols are the thermal unfolding curve based on Trp fluorescence at 340 nm and the solid line is the thermal unfolding curve based on CD measurements (molar ellipticity) at 222 nm. The thermal unfolding curves for F136W/IpgC and N341W/ IpgC are shown.

T_ms were used to determine the stability of different IpaC regions for IpaC associated with IpgC (Table 3). These fluorescence profiles manifest the expected curvilinear decrease in emission intensity with increased temperature followed by an abrupt increase in emission and a final decrease in signal (an example is shown in Figure 7). These fluorescence transitions appear biphasic perhaps reflecting some complex dissociation in addition to the structural changes seen by CD. It is noteworthy that, using 55 °C as an arbitrary cutoff temperature, residues showing the earliest evidence for thermally induced unfolding are at positions 40, 207, 226, 247, and 341. These are also the residues least affected or protected from the aqueous solvent by IpgC binding. While such properties could be attributed to IpgC-induced conformational changes, the overall pattern suggests that these residues are excluded from interaction with the chaperone. Based on these collective findings, IpgC clearly organizes and stabilizes IpaC structure. It may also be possible to suggest a tentative model for this translocator−chaperone interaction based on these data (see below).

DISCUSSION

Although the TTSS is a common virulence trait for several bacterial pathogens, *Shigella* is unique in that many of its important host cell subversion activities are possessed by its translocator proteins themselves rather than by late

effectors. Thus, understanding of the *Shigella* translocator proteins IpaC and IpaB has the potential to provide a more comprehensive understanding of bacterial TTSS-based communication with eukaryotic cells. Prior to their secretion, IpaB and IpaC associate with the cytoplasmic chaperone IpgC. This prevents IpaB and IpaC from interacting with each other and with the bacterial inner membrane, as well as their targeted degradation in the bacterial cytoplasm (*4*). Upon receipt of a secretion signal, IpaB and IpaC are released from IpgC within the context of the TTSA base to travel through the TTSA needle for delivery to the host cell membrane. Since the TTSA has an inner diameter of about 2.5 nm, it is postulated that the proteins must pass through the needle in a partially unfolded state (*27*). Despite the fact that IpaB and IpaC behave as membrane proteins and can aggregate when purified, some information concerning their membrane binding properties and invasion functions has been obtained (*10*−*13*, *15*, *23*, *28*). Unfortunately, structural data of any type has been difficult to obtain. Furthermore, in contrast to the class I chaperones where several high-resolution structures are available, information pertaining to the TTSS class II chaperones continues to be limited despite the potential for multiple functions, including transcriptional control (*6*, *20*).

In this study, IpaB and IpaC were coexpressed with their chaperone IpgC, permitting the purification of soluble and stable translocator/chaperone complexes. Multiple analyses demonstrate that IpgC interaction with the individual translocators gives rise to highly elongated heterodimers. This distinguishes them from the class I chaperone complexes. It was previously reported that *Pseudomonas aeruginosa* chaperone PcrH associates with the translocators PopB and PopD to form heterodimers (*20*), corroborating the results seen here.

Because of similarities with the *Pseudomonas* system, low pH was used to separate the translocator−IpgC complexes into their component proteins (*20*). Although this was successful for the IpaC/IpgC complex, release of IpaB from the IpaB/IpgC complex required OPOE, which is a mild detergent previously reported to aid in the extraction of recombinant IpaB from the *E. coli* membrane fraction (*22*). These data imply that the interactions between IpgC and the two translocators are distinct. It is intriguing that IpgC can independently interact with two proteins having no obvious sequence similarity using apparently unique intermolecular interactions. Edqvist et al. demonstrated a similar binding phenomenon with the *Yersinia* class II chaperone LcrH (*29*) Furthermore, it appears that the released IpgC can then associate with the transcription factor MxiE to cause activation of virulence gene expression (*30*, *31*).

CD analysis of the translocator/chaperone complexes and the individual proteins demonstrates that IpgC possesses a significant amount of α-helical structure while IpaB and IpaC possess somewhat greater disordered structure. Following its association with IpgC, there is a readily detectable increase in α-helical structure for IpaC, thus suggesting that chaperone binding is inducing significant secondary structure changes. Because IpaC lacks Trp residues, further studies involving Trp-scanning mutagenesis were limited to an examination of its interaction with IpgC. Trp fluorescence reveals significant impact of IpgC on various microenvironments throughout the IpaC molecule. IpgC binding did not greatly impact Trp residues within a functionally irrelevant region near the IpaC N-terminus (W40) nor Trp residues within a dispensable central hydrophilic region (W195, W207, W226, W270, W247) (*15*, *17*). The small blue shift exhibited by W40 and L207 (and possibly other positions) may be attributable to the proximity of the postulated IpgC binding site. In contrast, association with IpgC had a substantial impact on the residues lying within the hydrophobic region (W106 and W154) and on those of the C-terminal region (W362) including the predicted coiled-coil segment (W336 and W341) (*26*). It should be noted that the hydrophobic region is important for IpaC interaction with phospholipid membranes (*17*) and the C-terminal portion is key for IpaC oligomerization (*17*). These are among the functions blocked by IpaC association with IpgC.

While the interaction of IpgC with the hydrophobic region was expected, its apparent interaction with the C-terminus or, alternatively, the conformational change induced in this region upon IpgC binding was not. A Trp residue whose fluorescence undergoes a major blue shift in the IpgC complex is located at position 362. This residue is very important for IpaC's invasion function (*16*), but not for secretion or the insertion of functional IpaB/IpaC pores in erythrocytes. This implies that IpgC may not directly associate with this residue, but rather that it induces a structural change in the C-terminal tail of IpaC. This could also explain the conformational differences between the monomeric and oligomerized forms of IpaC. Likewise, the dramatic wavelength shift of W336 and W341 suggests that the tertiary structure within this region is influenced by chaperone binding. Alternatively, these fluorescence changes could be due to the localization of these residues at the IpaC−IpgC interface. Because the IpaC hydrophobic and C-terminal regions span a large distance within the IpaC primary sequence, it seems likely that IpgC mediates major global structural changes in IpaC or that the involved residues are located within an extended subunit interface between the two proteins.

Because of the narrow inner diameter of the TTSA secretion channel, IpaB and IpaC must be partially unfolded or special secretion-compatible structures found during their export. One role of the TTSS chaperones appears to be to maintain their partners in a secretion competent state within the bacterial cytoplasm, perhaps in such a partially unfolded conformation. Based on the data presented here, it is likely that the translocator/chaperone complexes are highly structured. The increased T_m upon IpgC interaction indicates that both IpaB and IpaC are significantly stabilized by their interaction with the chaperone. Based on the size differential between the two proteins, fluorescence emission data, and thermal unfolding data, we propose that IpaC possesses significant structure within the IpaC/IpgC complex. The main region involved in the IpaC−IpgC interaction seems to involve the IpaC central hydrophobic region and sequences immediately upstream along with regions near the IpaC C-terminus. Meanwhile, a major central hydrophilic region may not contribute greatly to this translocator/chaperone interaction although deletion of this region from IpaC reduces the overall α-helix content of the translocator/chaperone complex. This is supported by data involving the IpaCΔ mutant. Incorporating these data and taking the 1:1 stoichiometry findings into account, we thus envision a "looped"

form of IpaC that interacts with IpgC to temporally shield IpaC regions involved in IpaB interaction, membrane penetration, and self-oligomerization prior to TTSS export to the host cell surface. A similar interaction for the IpaB/IpgC complex may occur, but this will require additional detailed structural analysis to evaluate more critically.

A full understanding of the significance of the structural changes and stabilizing effects introduced to IpaB and IpaC by the class II chaperone IpgC warrants an exploration of the forces responsible for both complex association and dissociation. It is clear from this investigation that different physical influences (i.e., pH versus mild detergent) are needed to separate IpaB and IpaC from IpgC *in vitro*, but how this relates to the actual mechanism of type III secretion and the role of the TTSS Spa47 ATPase remains to be determined. Nevertheless, this first characterization of the structure and biophysical properties of a *Shigella* class II chaperone and its binding partners provides a starting point from which to better understand an important facet of type III secretion involving the presentation of TTSS translocator substrates to the secretion apparatus.

ACKNOWLEDGMENT

Technical assistance from Roma Kenjale, Sarah Rome, Ian Bales, and Lingling Zhang is gratefully acknowledged. Critical reading of the manuscript by members of the Picking lab is also acknowledged.

SUPPORTING INFORMATION AVAILABLE

Figure S1, which shows the protease sensitivity of IpaC alone and IpaC as part of the complex with its chaperone IpgC. This material is available free of charge via the Internet at http://pubs.acs.org.

REFERENCES

1. Hueck, C. J. (1998) Type III protein secretion systems in bacterial pathogens of animals and plants, *Microbiol. Mol. Biol. Rev. 62*, 379−433.
2. Cossart, P., and Sansonetti, P. J. (2004) Bacterial invasion: the paradigms of enteroinvasive pathogens, *Science 304*, 242−248.
3. Buttner, D., and Bonas, U. (2002) Port of entry—the type III secretion translocon, *Trends Microbiol. 10*, 186−192.
4. Menard, R., Sansonetti, P., Parsot, C., and Vasselon, T. (1994) Extracellular association and cytoplasmic partitioning of the IpaB and IpaC invasins of *S. flexneri*, *Cell 79*, 515−525.
5. Mavris, M., Page, A. L., Tournebize, R., Demers, B., Sansonetti, P., and Parsot, C. (2002) Regulation of transcription by the activity of the *Shigella flexneri* type III secretion apparatus, *Mol. Microbiol. 43*, 1543−1553.
6. Parsot, C., Hamiaux, C., and Page, A. L. (2003) The various and varying roles of specific chaperones in type III secretion systems, *Curr. Opin. Microbiol. 6*, 7−14.
7. Tran, Van Nhieu, G., Bourdet-Sicard, R., Dumenil, G., Blocker, A., and Sansonetti, P. J. (2000) Bacterial signals and cell responses during *Shigella* entry into epithelial cells, *Cell. Microbiol. 2*, 187−193.
8. Blocker, A., Gounon, P., Larquet, E., Niebuhr, K., Cabiaux, V., Parsot, C., and Sansonetti, P. (1999) The tripartite type III secreton of *Shigella flexneri* inserts IpaB and IpaC into host membranes, *J. Cell Biol. 147*, 683−693.
9. Tran Van Nhieu, G., and Sansonetti, P. J. (1999) Mechanism of *Shigella* entry into epithelial cells, *Curr. Opin. Microbiol. 2*, 51−55.
10. Zychlinsky, A., Kenny, B., Menard, R., Prevost, M. C., Holland, I. B., and Sansonetti, P. J. (1994) IpaB mediates macrophage apoptosis induced by *Shigella flexneri*, *Mol. Microbiol. 11*, 619−627.
11. Kueltzo, L. A., Osiecki, J., Barker, J., Picking, W. L., Ersoy, B., Picking, W. D., and Middaugh, C. R. (2003) Structure-function analysis of invasion plasmid antigen C (IpaC) from *Shigella flexneri*, *J. Biol. Chem. 278*, 2792−2798.
12. Marquart, M. E., Picking, W. L., and Picking, W. D. (1996) Soluble invasion plasmid antigen C (IpaC) from *Shigella flexneri* elicits epithelial cell responses related to pathogen invasion, *Infect. Immun. 64*, 4182−4187.
13. Tran Van Nhieu, G., Caron, E., Hall, A., and Sansonetti, P. J. (1999) IpaC induces actin polymerization and filopodia formation during *Shigella* entry into epithelial cells, *EMBO J. 18*, 3249−3262.
14. Picking, W. L., Mertz, J. A., Marquart, M. E., and Picking, W. D. (1996) Cloning, expression, and affinity purification of recombinant *Shigella flexneri* invasion plasmid antigens IpaB and IpaC, *Protein Expression Purif. 8*, 401−408.
15. Harrington, A. T., Hearn, P. D., Picking, W. L., Barker, J. R., Wessel, A., and Picking, W. D. (2003) Structural characterization of the N terminus of IpaC from *Shigella flexneri*, *Infect. Immun. 71*, 1255−1264.
16. Harrington, A., Darboe, N., Kenjale, R., Picking, W. L., Middaugh, C. R., Birket, S., and Picking, W. D. (2006) Characterization of the Interaction of Single Tryptophan Containing Mutants of IpaC from *Shigella flexneri* with Phospholipid Membranes, *Biochemistry 45*, 626−636.
17. Picking, W. L., Coye, L., Osiecki, J. C., Barnoski, Serfis, A., Schaper, E., and Picking, W. D. (2001) Identification of functional regions within invasion plasmid antigen C (IpaC) of *Shigella flexneri*, *Mol. Microbiol. 39*, 100−111.
18. Mach, H., Middaugh, C. R., and Lewis, R. V. (1992) Statistical determination of the average values of the extinction coefficients of tryptophan and tyrosine in native proteins, *Anal. Biochem. 200*, 74−80.
19. Vonderviszt, F., Imada, K., Furukawa, Y., Uedaira, H., Taniguchi, H., and Namba, K. (1998) Mechanism of self-association and filament capping by flagellar HAP2, *J. Mol. Biol. 284*, 1399−1416.
20. Schoehn, G., Di, Guilmi, A. M., Lemaire, D., Attree, I., Weissenhorn, W., and Dessen, A. (2003) Oligomerization of type III secretion proteins PopB and PopD precedes pore formation in *Pseudomonas*, *EMBO J. 22*, 4957−4967.
21. Tran, N., Serfis, A. B., Osiecki, J. C., Picking, W. L., Coye, L., Davis, R., and Picking, W. D. (2000) Interaction of *Shigella flexneri* IpaC with model membranes correlates with effects on cultured cells, *Infect. Immun. 68*, 3710−3715.
22. Hume, P. J., McGhie, E. J., Hayward, R. D., and Koronakis, V. (2003) The purified *Shigella* IpaB and *Salmonella* SipB translocators share biochemical properties and membrane topology, *Mol. Microbiol. 49*, 425−439.
23. De Geyter, C., Vogt, B., Benjelloun-Touimi, Z., Sansonetti, P. J., Ruysschaert, J. M., Parsot, C., and Cabiaux, V. (1997) Purification of IpaC, a protein involved in entry of *Shigella flexneri* into epithelial cells and characterization of its interaction with lipid membranes, *FEBS Lett. 400*, 149−154.
24. Lobley, A., and Whitmore, L.,Wallace, B. A. (2002) DICHROWEB: an interactive website for the analysis of protein secondary structure from circular dichroism spectra, *Bioinformatics 18*, 211−212.
25. Whitmore, L., and Wallace, B. A. (2004) DICHROWEB: an online server for protein secondary structure analyses from circular dichroism spectroscopic data, *Nucleic Acids Res. 32*, W668−673.
26. Pallen, M. J., Dougan, G., and Frankel, G. (1997) Coiled-coil domains in proteins secreted by type III secretion systems, *Mol. Microbiol. 25*, 423−425.
27. Cordes, F. S., Komoriya, K., Larquet, E., Yang, S., Egelman, E. H., Blocker, A., and Lea, S. M. (2003) Helical structure of the needle of the type III secretion system of *Shigella flexneri*, *J. Biol. Chem. 278*, 17103−17107.
28. Osiecki, J. C., Barker, J., Picking, W. L., Serfis, A. B., Berring, E., Shah, S., Harrington, A., and Picking, W. D. (2001) IpaC from *Shigella* and SipC from *Salmonella* possess similar biochemical properties but are functionally distinct, *Mol. Microbiol. 42*, 469−481.
29. Edqvist, P. J., Broms, J. E., Betts, H. J., Forsberg, A., Pallen, M. J., and Francis, M. S. (2006) Tetratricopeptide repeats in the type III secretion chaperone, LcrH: their role in substrate binding and secretion, *Mol. Microbiol. 59*, 31−44.

30. Mavris, M., Sansonetti, P. J., and Parsot, C. (2002) Identification of the cis-acting site involved in activation of promoters regulated by activity of the type III secretion apparatus in *Shigella flexneri*, *J. Bacteriol. 184*, 6751−6759.
31. Parsot, C., Ageron, E., Penno, C., Mavris, M., Jamoussi, K., d'Hauteville, H., Sansonetti, P., and Demers, B. (2005) A secreted anti-activator, OspD1, and its chaperone, Spa15, are involved in the control of transcription by the type III secretion apparatus activity in Shigella flexneri, *Mol. Microbiol. 56*, 1627−1635.
32. Provencher, S. W., and Glockner, J. (1981) Estimation of globular protein secondary structure from circular dichroism, *Biochemistry 20*, 33−37.
33. Sreerema, N. W., and R. W. (1990) A self-consistent method for the analysis of protein secondary structure from circular dichroism, *Anal. Biochem. 209*, 32−44.

BI700099C